THE AHUACAPAN GEOTHERMAL FIELD AFTER 20 YEARS OF EXPLOITATION

D.Amore F.* and Montalvo F.#

* **International Institute for Geothermal Research, Pisa, Italy**

Comisión Ejecutiva Hidroeléctrica del Rio Lempa (C.E.L.), El Salvador

ABSTRACT

A study of the physical and chemical data of Ahuachapan field, during 20 years of production allows a formulation of the conceptual model of the field. Chloride content, SiO_2 and Na-K-Ca temperatures, Cl/SO_4 ratio,, enthzlpy-chloride relations and gas geothermometry have been used to understand the **main** phenomena affecting the observed fluid compositions. The main phenomena can be summarized as due to:

1) an upflow zone located in the South **part** of the field with a **fluid** moving **laterally mostly** North at different depths from **500** to **1000** m ;

2) a shallow rescharge, at depth of the order of 500 m, **of** diluted water **from E-NE of** a metheoric water due to lowering of the pressure in the original reservoir ;

3) a deep rescharge made of an andesitic acidic and gassy fluid from depth ;

4) local boiling.

INTRODUCTION

A general review of the chemical changes which have occurred in the reservoir of Ahuachapan geothermal field **(Figs** 1 and 2) is given with emphasis on the main processes resulting from intensive mass extraction in twenty years of commercial exploitation. The Ahuachapán geothermal field has been monitored systematically since 1975 when continuous power generation started. Table **1** reports the general characteristics of production wells, as Table 2 reports the production characteristics of the wells **at** starting and actual conditions. Data are reported as annual average. We can recognize same wells showing at present high

values of enthalpy and in particular wells AH-6, AH-17 and AH-26 which are centers of boiling. The field totalized less than 70 MWe in 1996. The decline in energy production after 20 years, is about 30%. Previous studies for Ahuachapan geothermal field are in Truesdell et al. 1989, Steingrimsson et al. 1991, Montalvo 1994 and D'Amore 1996. Fig. 3 shows the possible upflow zone located close to the Laguna Verde with the lateral flow of the fluid toward N-NE. It shows also the position of the recharge from above located in the N-NE zone close to Chipilapa field. The natural manifestations in the South zone, are mostly represented by fumaroles and steam vents. The outflow can be located North close to El Salitre NaCl spring.

WATER CHEMISTRY EVOLUTION

The main hot fluid recharge comes from the South near the Laguna Verde andesitic volcanic complex and moves through the field mixing with cold water inflow from above mainly in the SE part. Due to the fault system, the main recharge from the upflow zone reaches the SW part as undiluted fluid, as indicated by the salinity and geothennometer temperatures that are almost the same as original values (near 9000 mg/kg and 240°C respectively). The field is mainly recharged by two fluids: a hot deep fluid rich in gas and sulfates with low pH, and a natural recharge flowing from above. The cold water recharge, after interaction with rock, becomes a fluid with a moderate salinity and temperature (1000 ppm, 160°C; Montalvo, 1994). The effects of dilution are evidenciated using reservoir chloride concentration (Figs. 4 to 6) showing the areal distribution of chloride content in 1975, 1985 and in 1995 respectively. It is evident an increasing dilution due to recharge water from ENE and a resistance to dilution in the W-SW zone, probably close to where the upflow zone is located (near well AH-31). Figs. 7 and 8 show the areal distribution of T_{SiO2} in 1978 and in 1995. It evidences a strong decline in temperature in the N-NE zone with the highest computed temperatures in the S-SW zone. The areal distribution of the Na-K-Ca temperatures at starting conditions and in 1995 evidenciate a maximum of temperature located close to well *AH-31*, which can be the most representative of the upflow zone (Fig. 9).

The dominant reservoir processes of the Ahuachapan field due to exploitation without reinjection are dilution from the cold water recharge from NE, deep recharge and boiling.

The dilution and decline in reservoir enthalpy characterize wells in the northern and northeastern sectors of the wellfield. In the south and southwest, however, stable conditions are observed. General decrease of the Cl/SO_4 ratio is observed as due to lateral dilution and decline in chloride content and constant or increasing values of sulfate. The increase in sulfate

concentration can not be due to cooling of fluid by dilution, because anhydrite is not a primary mineral in andesitic systems. We have than to infer a deep source for sulphate.

During exploitation a decrease in pH of one unit in average and increase of computed partial pressure of CO_2, H_2 and H_2S in almost all wells up to 8 times were observed. The only explaination of this is consistent with an inflow from beneath the productive horizon of an hot acidic and gassy fluid.

The cationic geothermometers results show in general a clear cooling trend up to 1985-87 and stabilization and recovery after that. This is possible related to the inflow of some deep recharge fluid in the local aquifer in recent time.

The silica geothermometer, however, also shows an initial decline but followed by an abrupt increase from around 1985-1987 to 1991 when decline started again. This may be related to boiling that increases the silica concentrations followed by renewed dilution.

The average of Na/K temperatures range between 230-250°C and those of Na-K-Ca between 240-255°C. The cationic geothermometers are not strongly affected by the process of metheoric water dilution and the relatively fast cooling of the system. The relative position of the observed trend seems to be related to different feed zones: a shallow one above 500 m, and a deeper horizon around 1000 m. The lower cationic geotemperature are in general observed for the shallow wells.

Figs. 10 to 14 show for some typical wells the enthalpy-chloride diagram. Different phenomena can explain the trends with time: conductive heat gain and heat losses (or dilution + boiling) can move the points respectively up or down. Dilution in the formation moves the points on the left at constant enthalpy. Common phenomena at Ahuachapan are steam gain, moving the points up-left at 45°, and dilution in the well moving the point down-left at 45°. Both phenomena induce dilution represented by a decrease in Cl with respectively an increase or a decrease in enthalpy. For most of the wells, some of these phenomena can explain the observed temporal evolution. For example, shallow well *AH-6* shows (Fig.11) at first an increase in enthalpy due to conductive heating and than steam gain + boiling: both phenomena increase the chloride content and the enthalpy up to 1992. Then a local dilution in the wells, with cooling of the local aquifer, can explain the decrease of both enthalpy and chloride content. Reservoir chloride and measured discharge enthalpy for low and moderate enthalpy wells is shown, but for high-enthalpy wells the enthalpy calculated from Na-K-Ca geothermometer temperatures is used. It is shown a clearly typical dilution for some of the low enthalpy wells, which causes a decrease in enthalpy and chloride with time because of dilution from relatively cold water. A complex trend is evident for the high enthalpy wells that could be related to boiling and heat transfer combined with cooling and dilution processes. In the vicinity of a particular well several mechanism can be assumed to explain

the different tendencies described above. Boiling, heat transfer from the rock and steam addition can change the enthalpy without changing the chloride (Truesdell et al., 1988).
The enthalpy evolution of Ahuachapdn production wells is revealed by the comparison between the measured enthalpy and the liquid-phase enthalpy values calculated from geothermometer temperatures. Boiling lowers fluid temperatures within expanding boiling zones with progressively decreasing pressures as the fluid follows the two-phase liquid-vapor curve. The near-well fluid is cooled by boiling, and heat is transferred to the fluid from the reservoir rocks, probably as a result of flashing flow in fractures. Fig. 15 shows for two wells the measured enthalpy and the values of enthalpy for a liquid phase computed from Si02 and Na-K-Ca geothermometers vs. time. We can recognize two main different types of trend: when the measured enthalpy is higher than other two, and when the measured enthalpy is lower than other two. In the first case we have heat transfer from the rock and boiling, and in the second case, we have dilution from cooler water.

GAS-WATER-ROCK INTERACTION PROCESSES

The study of saturation indexes evaluates thermodynamic equilibria between the aqueous solution and possible alteration hydrothermal minerals. The WATCH code (Amorsson, 1982, Bjarnason, 1994), was used taking into consideration the phenomena of flashing and degassing. The computed reservoir water for selected wells is reported in Tables 3 and 4 at starting conditions and in 1995. The degassing was considered at the separator temperatures. The saturation index is defined as SI = log(Q/K), where Q is the solubility product for a given reaction involving a mineral, and K is the equilibrium constant of the hydrolisis reaction at the same temperature. Equilibrium can be obtained for SI values equal 0 ± 0.25 and for pyrite 0 ± 5. The choice of the possible alteration mineral to be considered was made easier by the petrographic study of cuttings for the wells. The following mineral species have been considered: calcite, pyrite, quartz, wairakite, laumontite, prehnite, zoisite, epidote, muscovite, diopside, microcline and low-albite. We also add anhydrite to explain SO4 content and diopside to explain Mg content. Indeed, the system is undersaturated in Mg-chlorite and amphiboles at all temperatures. The locally found chlorite is of the Mg-Fe solid solution type and not fraction of Fe was at the moment available to calculate the constant of equilibrium. Anhydrite can be probably present only at the points of loss of circulation (not available for petrographical study). After several years of production, most of the initially at equilibrium minerals become undersaturated with exception of anhydrite, quartz, laumontite, low-albite and K-feldspar at temperature lower than 210°C. Figs 16 shows the values of SI vs temperature for several minerals at starting conditions for the well *AH-6*.

The application of the method produces the following results:

a) The alteration mineral paragenesis is consistent with the mineral found in the cuttings at depth. At beginning of production computed temperatures for SI = 0 for all wells are between 230 and 240°C.

b) The generated temperatures from the use of SI values are consistent with the masured values both at the starting production conditions and in 1995 (Fig. 17). Following average temperatures can be calculated for well A6 (Figs 16) 233±4°C at starting conditions and 205±7°C in 1995. The general lowering of the computed temperatures for all wells is consistent with the general dilution and cooling in the convective shallow production zone of the reservoir, due to inflow of shallow diluted recharge meteoric water. Most of the initial alteration minerals become undersaturated. This is due to the different rates of reequilibration for each mineral in the water-rock interaction process. This means that quartz and anhydrite reequilibrate faster that laumontite and Na-K-feldspars, and these faster then the other sylicates.

c) If we look at the reservoir data generated by WATCH code we note that calcite at initial condition was saturated (average saturation index of calcite equal to 0.15±0.3), and in 1995 was undersaturated with an average saturation index of calcite equal to -0.9±0.4. This means that the available contents of Ca^{2+} and CO_3^{2-} are not sufficient to produce saturation in the reservoir at a temperature of the order of 205-220°C. This is mostly due to the lowering of the pH values. When during rising of the fluid the temperature of the solution decreases down to about 160°C, considering the increase of the value of equilibrium constant for calcite dissociation, we obtain as a final results a very large negative value of saturation index (<-1). This means absolutely no scaling up to separator.

d) In the reservoir computed composition we observe the following changes after about 20 years of production considering all wells:

the pH measured values decrease from an original valur of 7.3± 0.06 to an actual value of 6.5±0.4. Considering the deep reservoir water the average pH declines from about 5.9 to about 5.0;

SiO_2 content decreases from an original value of 424±43 mg/l to a final value of 360±49 mg/kg;

the Cl content decreases from an original value of 8555605 mg/kg to a final value of 724521023 mg/kg in the reservoir;

the average boron content behaves exactly as chloride with a decrement close to 15%;

SO4 content increases from an original value of 28±6 mg/l to a final value of 3328 mg/kg despite the dilution;

CO_2 partial pressure increases from a minimum of 0.03 Mpa to a maximum of 0.3 Mpa.

H_2S partial pressure increases from a minimum of 0.0008 MPa to a maximum of 0.003 MPa. H_2 partial pressure increases in average from 0.002 to ***0.006*** MPa.

Table 5 shows the computed variations **of** selected parameters between initial conditions and 1995 for **7** selected wells.

All these variations with time can be explained using a simple model based on a lateral input of diluted fluid with a temperature not exceeding 160°C (Montalvo,1994) due to the natural recharge to balance the local lowering of pressure due to exploitation wthout reinjection in the productive shallow zone of the reservoir, and a vertical input due to an exotic volcanic deep acidic gassy and salty fluid probably equilibrated at high temperature close to 300°C (as suggested by gas composition in the next section). This means also that we infer that the reservoir exploitable volume in Ahuachapan is much larger at depth that supposed fiom previous models.

GAS CHEMISTRY

Following observations can be made, considering the observed variations with time of the compositions:

1. Figs. **18,** 19 and 20 show respectively the CO_2, H_2S and H_2 contents in total discharge vs time. It is evident a general increment, despite theinflow of metheoric water from above.
2. Fig. 21 shows the gas/water ratios in the exploited area in 1995. The maximum are located in the boiling centers.

3. Using the method of D'Amore and Truesdell, 1985, Figs 22 and 23 shows the reservoir parameters temperature and steam fraction computed from starting conditions to 1995 for well AH-1 and AH-6. Well *AH-6* has a computed temperature up to 290°C in 1995 and its gas composition can be considered that best representing the deep source. It can be inferred that the temperature of the fluid stored in the deep volume of the reservoir (in andesitic rocks) would exceed 300°C. The contribution of the deep source **is** clarified considering the temperatures for each well in the following order (considering the minimum and the maximum computed temperatures):

AH-1	temperature range between 200 and 225°C,
AH-20	between 235 and 255°C,
AH-21, AH-23 and ***AH-27***	between 250 and 270°C,
AH-6, AH-17 'and AH-31,	,between275 and 300°C.

4. Using a new method based on gas composition including **NH3** and N_2 (D'Amore and Truesdell, **1997,** in prep.) it is possible to compute reservoir temperature, steam fraction and CO_2 partial pressure. Following three chemical equilibria equations have been considered:

$$CH_4 + 2H_2O = 4H_2 + CO_2$$
$$H_2 + 3/2FeS_2 + 2H_2O = 3H_2S + 1/2Fe_3O_4$$
$$N_2 + 4H_2 + 3/2FeS_2 + 2H_2O = 3H_2S + 2NH_3 + 1/2Fe_3O_4$$

Fig 24 shows the results vs time for well AH-6. It evidenciate an increase of the **three** reservoir parameters with time.

5. Different geothermometers were **used** at starting production and at present conditions (Figs. 25 and 26). Temperatures from SiO_2 geothermometer, temperatures generated from **WATCH** code and measured temperatures show a decrease (of about 20°C) due to the inflow of the recharge water. Temperatures computed from Na-K-Ca and Na/K remain almost constant as order of magnitude (in the range 240-250°C). Gas geothermometer D'Amore and Panichi, 1980, and results from the gas grid method show constant values or increased up to 290°C. The phenomenon of increase with time in reactive gas content **and** the gas partial pressures together **with** computed Steam fraction y and the temperature is quite peculiar of Ahuachapan field. Wairakei field for example shows with production and boiling strong decrease of gas content down to very negative y values (Giggenbach, 1980). Then as Wairakei is characterized by a reservoir sealed at bottom and laterally open to recharge, Ahuachapan reservoir (0.5-1.2 km) is open both to an input of recharge of water from above and of deep recharge. Similar behavior characterize wklls of Palinpinon field (in the Philippines) located close to the local heat source (D'Amore et al, 1993).

5. Fig. 27 shows the temperature computed by the use of CO in the system CO_2-CO-CH_4. In 1995-1996 the values of CO were available. To compute the reservoir parameters, the following chemical reaction was considered :

$$CH_4 + 3CO_2 = 4CO + 2H_2O$$

Temperatures are between 250 and 300°C in a pure liquid phase.

6. The relative contents of Ar - N_2 - He are reported in a triangular diagram (Fig. 28) There **is** evidence for the gas a partial **origin** (in average 50%) from an andesitic magma. This is inferred because of the high ratios of both N_2/Ar and N_2/He. In the diagram it is supposed a pure meteoric origin for argon. He is supposed to be originated from mantle.

CONCLUSIONS

The conceptual model of Ahuachapan field, as function of the observed time variations of chemical and physical parameters can be outlined as follows.

The upflow zone can be located close to well AH-31 in the south near the Laguna Verde volcanic complex. The fluid than moves towards north through the exploited field mixing with cold water inflow from above mainly from SE (Chipilapa field). The **mixing** probably occurs at a depth of the order of 500 m, that is in the shallow zone of the exploited field. Due to the fault system, the main recharge from the upflow zone reaches the **SW** part as undiluted fluid, as indicated by the salinity and geothermometer temperatures that remain almost the same as original values (chloride content close to 9000 mg/kg and 240°C respectively). Cooling effects are evidenciated from temperature of silica in the reservoir. Some spots of intensive boiling can be located in the center of the field in shallow wells, producing a high enthalpy fluid.

The field is now mainly recharged by two fluids: a hot deep fluid rich in gas and sulfates with low pH, and natural recharge neutral water flowing from above (SE zone). The effects of dilution and cooling are evidenciated using reservoir chloride and silica concentrations It is evident an increasing dilution due to recharge water from ENE and a resistance to dilution in the W-SW zone, probably close to where the upflow zone is located (well AH-31). The value of temperature of the deep recharge can be evaluated close to 300°C using gas compositions. Fig. 27 shows the conceptual model of the field.

REFERENCES

Arnorsson **S.,** Sigurdsson **S.** and Svavarsson H. 1982. The chemistry of geothermal waters in Iceland. I. Calculation of aqueous speciation from 0°C to 370°C. Geochim. Cosmochim. Acta,46, 1513-1532.

Bjarnason J.O., 1994. The speciation program WATCH, version 2.0. Orkustofnun, Reykjavik.

D'Amore F. and Truesdell A.H. 1985. Calculations of geothermal reservoir temperature and steam fraction from gas composition. Geotherm. Resour. Counc. Trans., 9,305-310.

D'Amore F., Ramos-Candelaria M.N., Seastres Jr., J.S., Ruaya J.R. and Nuti **S.** 1993. Applications of gas chemistry in evaluating physical processes in the Southern Negros (Palinpinon) geothermal field, Philippines, Geothermics, 22,535-553.

D'Amore F. 1996. Isotope Hydrogeology and Geochemistry in geothermal fields. **IAEA** Technical Report El Salvador Mission. Project CEL ELS/8/005.

Giggenbach W.F. 1980. Geothermal gas equilibria. Geochimica Cosmochimica Acta, **44,** 2021-2032.

Montalvo F. 1994. Geochemical Evolution of the Ahuachapan geothermal field, El Salvador. Number 9 report. The United Nation University, Geothermal Training Programme, Iceland.

Steingrimsson B., Aunzo Z., Bodvarsson G.S., Truesdell A.H., Cuellar G., Escobar C. and Quintanilla A. 1991. Changes in thermodynamic conditions of the Ahuachapan reservoir due to production and injection. Geothermics, 20, 23-38.

Truesdell **A.H.,** Aunzo Z., Bodvarsson ***G.S.,*** Alonso J. and Campos **A.** 1989. The **use** of Ahuachapan chemistry to indicate natural state conditions and reservoir processes during exploitation. Proceedings of the 14th Workshop on Geothermal Reservoir Engineering, Stanford University, **USA,** 273-278.

TABLE 1: General characteristics of Ahuachapán production wells. Earlier and actual aquifer temperature is a downhole average measured at the feedpoints; TP: two phase aquifer, L: liquid aquifer (data from LBL, **1989;** and CEL, **1994)**

Well	Year drilled	Depth (m)	Casing 9 5/8" OD (m)	Earlier and Actual Aquif.Temp. (°C)	Main Aquifer (m)	Steam Fract. %	Power MWe
AH-1	1968	1195	486.46	239-214	500^{TP} -550^{L}	10	3.3
AH-6	1970	591	454.3	232-209	480^{TP} -550^{TP}	78	4.4
AH-7	1970	950	483.36	226-220	520^{TP} -750^{L}	13	3.1
AH-17	1976	1200	450	225-205	468^{TP} , 870^{L}	100	6.1
AH-19	1978	1415	676	231-224	700^{TP}, 1100^{L}	14	3.5
AH-20	1974	850	450	220-205	460^{TP} -500^{TP}	20	5.8
AH-21	1975	849	500	227-210	500^{TP} -600^{L}	15	7.1
AH-22	1975	660	508.8	235-214	520^{TP} -600^{L}	34	2.6
AH-23	1977	924	459.5	224-215	460^{TP} -525^{TP}	22	4.5
AH-24	1976	850	411	223-209	452^{TP} -650^{L}	15	3
AH-26	1975	804	399	226-202	411^{TP} -650^{L}	43	2.8
MI-27	1978	800	412	235-219	425^{TP} -750^{L}	25	7.4
AH-28	1978	1000	428	227-224	450^{TP} -850^{L}	13	4.6
AH-31	1981	1502	489.8	232-225	560^{TP} -1000^{L}	14	6.1
AH-32	1985	1504	487.5	240-237	800^{TP} -1000^{L}	14	5.4

TABLE 2 production characteristics at starting and actual conditions for the production wells at Ahuachapan geothermal field (annual average)

Wells	Year	Steam (kg/s)	Water (kg/s)	Total (kg/s)	Hm (kJ/kg)	WHP (kg/cm2a)	Ysep	Pot. MWe
AH-1	1977	14.3	74.2	88.5	1004	6.3	0.16	5.3+2
	1995	6.6	48.4	55.0	919	6.05	0.12	3.30
AH4	1977	17.9	42.6	60.6	1308	6.4	0.30	7.10
	1995	11.6	5.9	17.5	2051	6.05	0.66	4.60
AH-7	1977	8.6	51.2	59.8	838	6.3	0.14	3.30
	1994	5.7	35.1	40.8	954	5.87	0.14	3.10
AH-17	1981	30.9		30.9	2763	7	1.00	7.00
	1995	17.05	0.18	17.19	2825	11.90	0.99	6.80
AH-19	1984	6.3	47.5	53.8	931	10.29	0.12	2.6+1.5
	1994	6.4	41.2	47.6	949	9.23	0.13	3.50
AH-20	1977	11.1	44.0	55.1	1101	8.7	0.20	4.8+1.3
	1995	12.6	58.2	70.7	1043	6.95	0.18	6.20
AH-21	1978	12.2	59.5	71.6	995	8.7	0.18	5.8+2.8
	1995	12.6	78.0	90.7	965	7.78	0.14	6.70
AH-22	1977	15.9	49.8	65.7	1146	6.4	0.24	7.5+1.3
	1995	5.8	12.6	18.4	1327	5.94	032	2.60
AH-23	1980	9.0	47.3	563	1009	6.5	0.16	3+1.1
	1995	8.4	213	29.7	1253	5.91	0.28	3.80
AH-24	1978	8.23	44.27	52.50	994	6.3	0.16	3.8+0.9
	1995	4.50	30.10	34.60	937	5.95	0.13	2.40
AH-26	1977	11.3	22.1	33.4	1381	6.2	0.34	5.00
	1995	8.3	11.7	19.9	1534	5.96	0.42	3.30
AH-27	1980	24.0	59.4	83.4	1281	6.4	0.29	9.6+1.6
	1995	14.1	44.7	58.8	1167	5.9 1	0.24	6.60
AH-28	1980	24.0	71.0	95.0	1210	6.4	0.25	9.6+1.8
	1994	7.4	49.6	57.0	942	6.20	0.13	4.00
AH-31	1985	9.9	65.0	74.9	971	7.11	0.13	4.1+1.8
	1995	11.1	69.8	80.9	962	6.28	0.14	5.90

Table 3. Reservoir computed water composition (mg/kg) at initial production conditions (from WATCH code).

well	AH-1	AH-6	AH-20	AH-21	AH-23	AH-27
T res (°C)	228	233	233	230	234	245
pH	6.3	5.9	5.4	5.9	5.3	5.4
c 0 2	78.9	281	552	149	701	827
H2S	4.4	21.7	12.9	10.6	19.5	20.6
NH3	0.22	0.9	0.99	0.32	0.27	1.05
H2	0.01	0.05	0.16	0.02	0.035	0.06
CH4		0.02		0.04		0.016
N2		1.46	3.04	4.4	5.53	2.54
B	111	117	111	128	110	119
Si02	430	383	388	406	435	501
Na	4637	4767	4397	5111	4289	4705
K	760	783	672	848	639	835
Mg	0.113	0.07	0.069	0.06	0.06	0.04
Ca	388	389	399	402	373	340
F	0.83	0.547	0.842	0.756	0.97	0.82
Cl	8410	8745	8171	9355	7929	8730
SO4	26.8	30.1	34.3	22.8	33.2	19.1
Al	0.013	0.013	0.013	0.013	0.013	0.012
Fe	0.044	0.043	0.042	0.043	0.043	0.041
TDS	14779	15242	14192	16289	13829	15272
P(CO2) bar	0.17	0.654	1.47	0.367	1.9	2.11
P(H2S) bar	0.409 E-2	0.214 E-1	1.40E-02	1.10E-02	2.11E-02	2.12E-02
P(NH3) bar	0.434 E-4	0.144 E-3	0.01 E-3	0.528 E-4	0.275 E-4	0.142 E-3
P(H2) bar	0.233 E-2	0.152 E-1	0.488 E-1	0.554 E-2	0.12 E-1	0.518 E-1
P(CH4) bar		0.217 E-3		0.217 E-2		0.779 E-2
P(N2) bar		0.378 E-1	0.804 E-1	0.121	0.145	.0181 E-1
P(H2O) bar	26.9	29.5	29.5	28	30.1	36.5
log P(O2)	-37.6	-39	-39.7	-38.2	-38.3	-37.4
log P(S2)	-12.8	-13.1	-14.4	-12.1	-12.8	-12.7
T meas.(°C)	230	235	225	230	230	240
T quartz (°C)	241	230	233	236	243	258
T Si02 (°C)	231	225	220	231	227	240
T Na-K-Ca (°C)	246	253	245	256	243	260

NOTE: T res. is the temperature computed from the S.I. values of the alteration minerals in equilibrium with the brine in the reservoir. T meas. is the maximum temperature measured in the formation. At initial conditions, the temperature of the brine *can* be considered equal to the formation temperature. T quartz is generated by WATCH code. T Si02 is computed from data at weirbox.

Table 4. Reservoir computed water composition (mg/kg) at actual (1995) production conditions (from WATCH code).

well	AH-1	AH-6	AH-20	AH-21	AH-23	AH-27
year	1994	1995	1995	1995	1995	1995
T res (°C)	208	205	203	223	215	211
pH	5.6	4.9	5.3	5.3	4.6	5.0
CO2	104	805	271	370	1098	989
H2S	9.26	22.2	10.8	15.2	22.0	22.4
NH3	0.28	1.49	1.30	0.38	1.55	0.97
H2	0.14	0.15	0.11	0.15	0.18	0.16
CH4	0.24	0.21	0.20	0.29	0.33	0.33
N2	2.28	6.45	2.6	3.0	13.8	8.3
B	92	122	100	124	90	108
Si02	360	291	337	366	364	441
Na	3478	4528	3746	4683	3357	4030
K	578	717	593	841	525	724
Mg	0.110	0.110	0.156	0.09	0.107	0.09
Ca	242	402	289	337	226	247
F	1.16	1.62	1.38	1.68	1.32	1.60
Cl	6432	8332	6777	8548	6035	7347
SO4	34.9	42.4	38.1	23.0	32.4	24.7
Al	0.013	0.013	0.014	0.013	0.013	0.013
Fe	0.045	0.046	0.046	0.045	0.043	0.045
TDS	112233	14455	11889	14937	10638	12943
P(CO2) bar	0.293	2.420	0.805	1.039	3.270	2.950
P(H2S) bar	0.107 E-1	0.273 E-1	0.132 E-1	0.173 E-1	0.265 E-1	0.272 E-1
P(NH3) bar	0.202 E-4	0.254 E-4	0.376 E-4	0.247 E-4	0.181 E-4	0.132 E-4
P(H2) bar	0.569 E-1	0.698 E-1	0.465 E-1	0.523 E-1	0.673 E-1	0.646 E-1
P(CH4) bar	0.163 E-1	0.178 E-1	0.145 E-1	0.173 E-1	0.220 E-1	0.229 E-1
P(N2) bar	0.795 E-1	0.267	0.947 E-1	0.921 E-1	0.464 E-1	0.29
P(H2O) bar	18.3	17.2	16.2	24.5	21.0	19.5
log P(O2)	-43.5	-43	-43.3	-40.1	-42.1	-42.7
log P(S2)	-15.7	-15.2	-15.6	-14.7	-14.8	-14.9
T meas.(°C)	210	205	200	225	210	210
T quartz (°C)	225	208	220	228	227	245
T Si02 (°C)	219	204	212	213	221	234
T Na-K-Ca (°C)	252	247	246	260	248	260

NOTE: T res. is the temperature computed from the S.I. values of the alteration minerals in equilibrium with the brine in the reservoir. T meas. is the temperature of the brine and not the formation temperature. The last one is generally higher than the brine temperature because of the mixing with the recharge water. T quartz is generated by WATCH code. T Si02 is computed fiom data at weirbox.

Table 5 .Computed variations of selected parameters between initial conditions and 1995 for 7 wells of Ahuachapan.

Parameter	AH-1	AH-6	AH-20	AH-21	AH-23	AH-27	AH31
-A T RES	20.0	28.0	10.0	7.0	19.0	34.0	5.0
-A Cl RES %	31.0	5.00	21.0	9.0	31.0	19.0	17.0
A P CO2 %	72.0	270	-45.0	183	72.0	40.0	74.0
A P H2S %	162.0	28.0	0.0	57.0	26.0	28.0	117
Δ P H2 %	2342	359	-5.0	844	461	25.0	2.0
A (P CO2 / P HZO) %	153.0	535	0.0	224	147	162	90.0
-A (CI/ SO4)%	69.0	48.0	34.0	10.0	28.0	54.0	16.0
-A pH	0.70	1.00	0.10	0.60	0.70	0.40	1.30

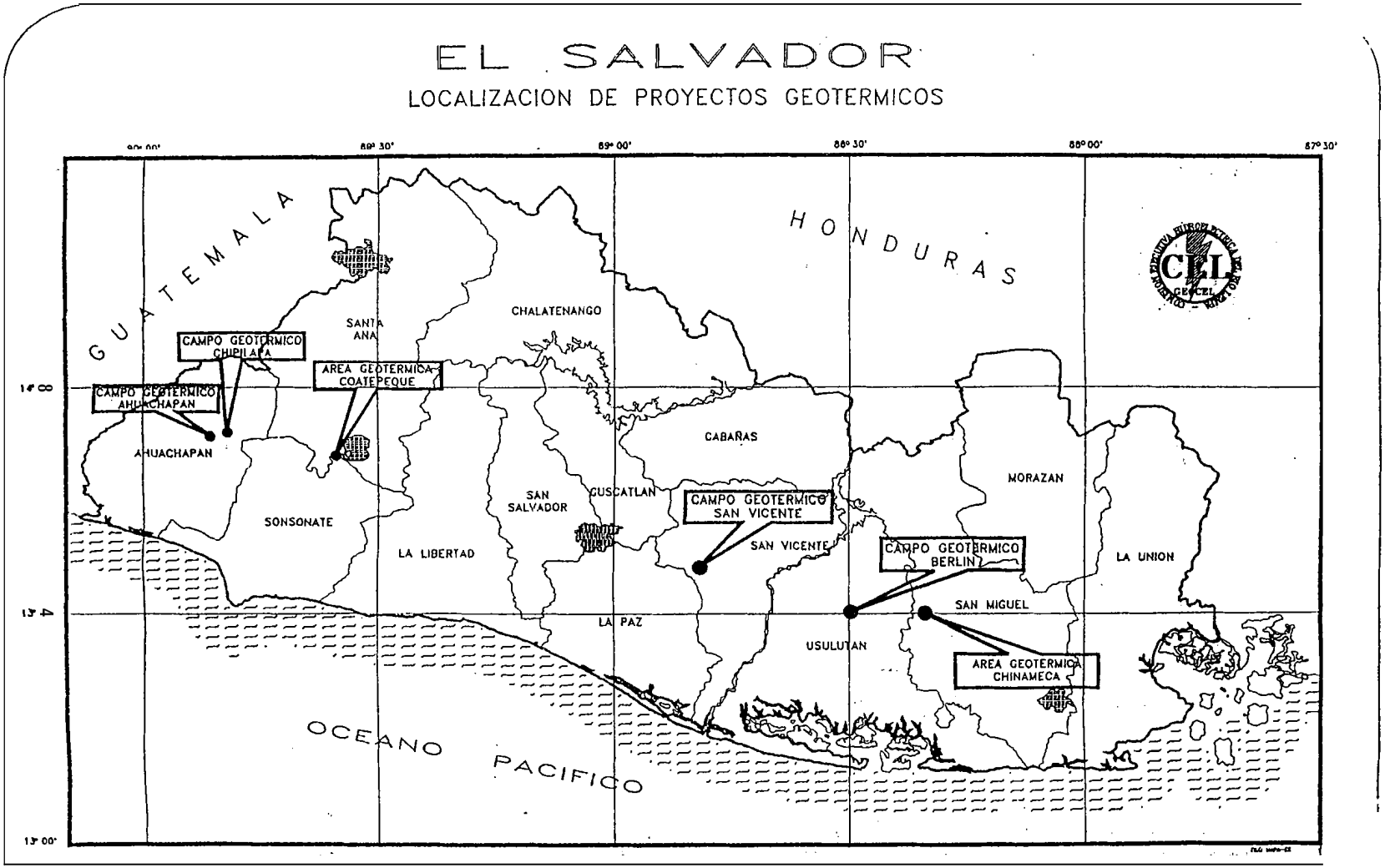

Fig.1 Localization of the geothermal projects in El Salvador.

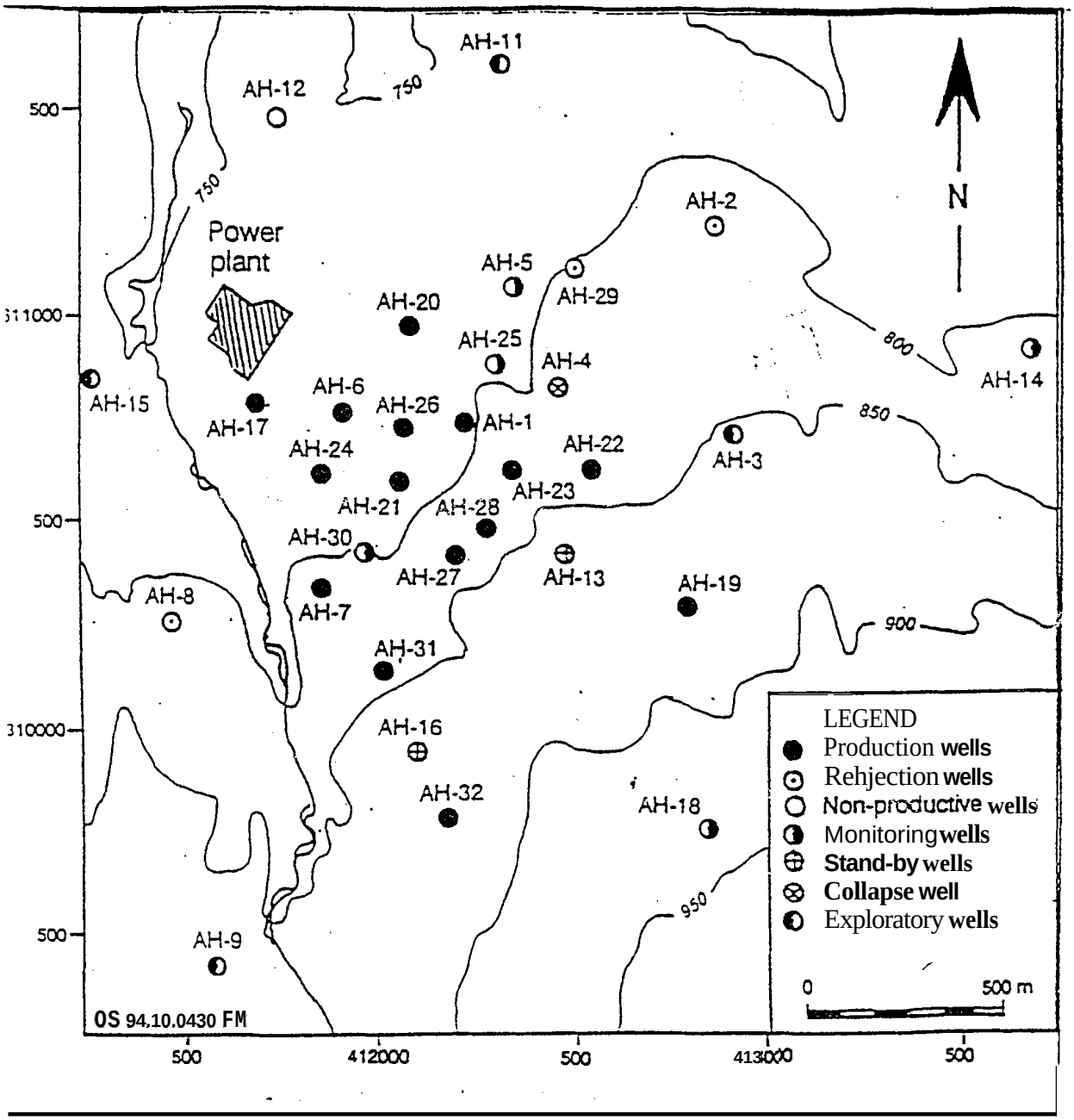

Fig.2 Well distribution in Ahuachapán geothermal field.

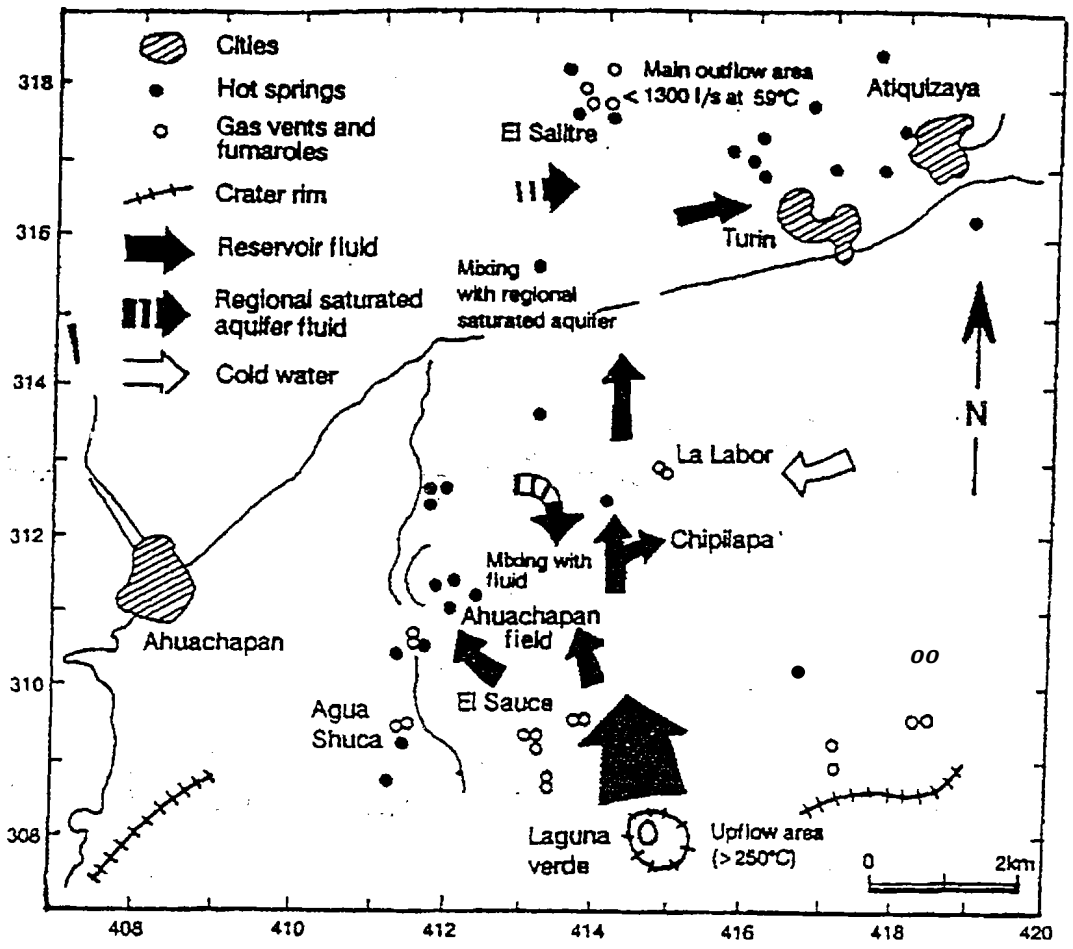

Fig.3 Possible upflow zone located close to the Laguna Verde with the lateral flow of the fluid toward N-NE. It shows also the position of the recharge from above located in the E-NE zone close to Chipilapa. The natural manifestations in the South zone, are mostly represented by fumaroles and steam vents. The downflow can be located North close to El Salitre NaCl spring.

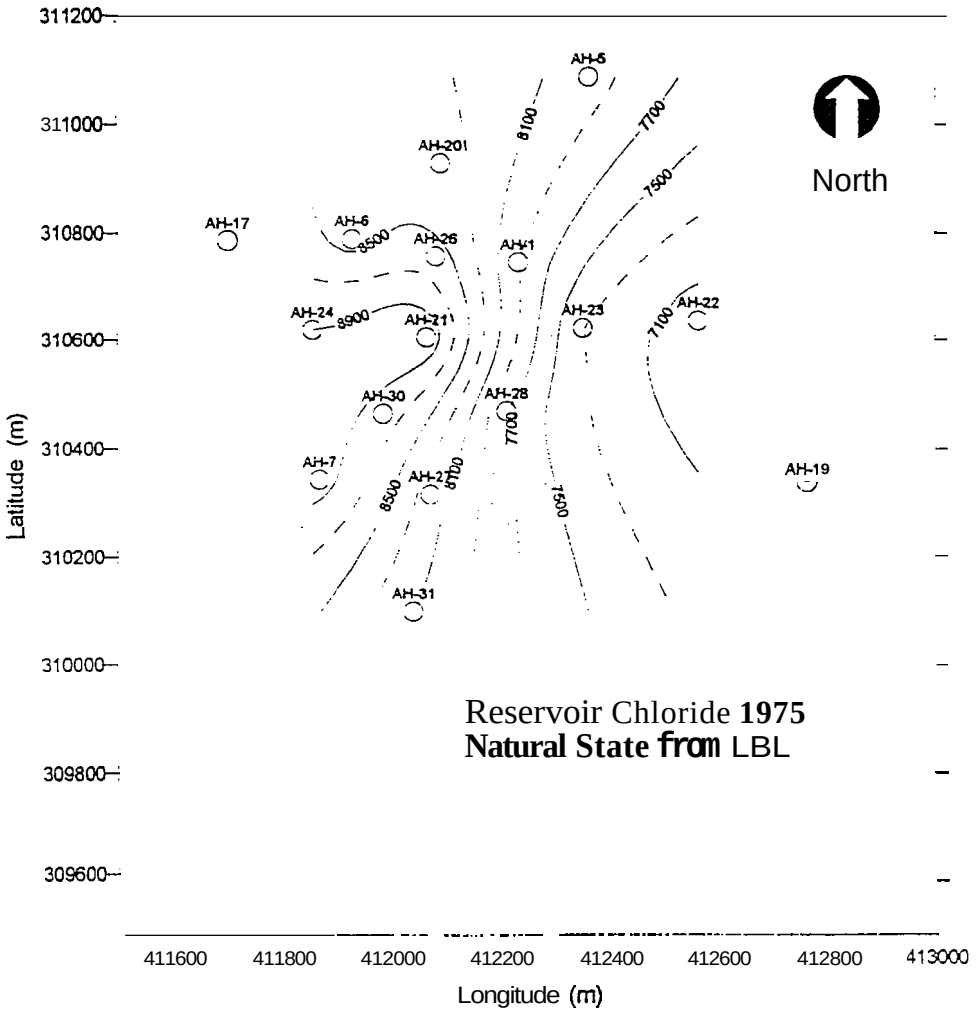

Figs. 4 Areal distribution of chloride content at starting conditions

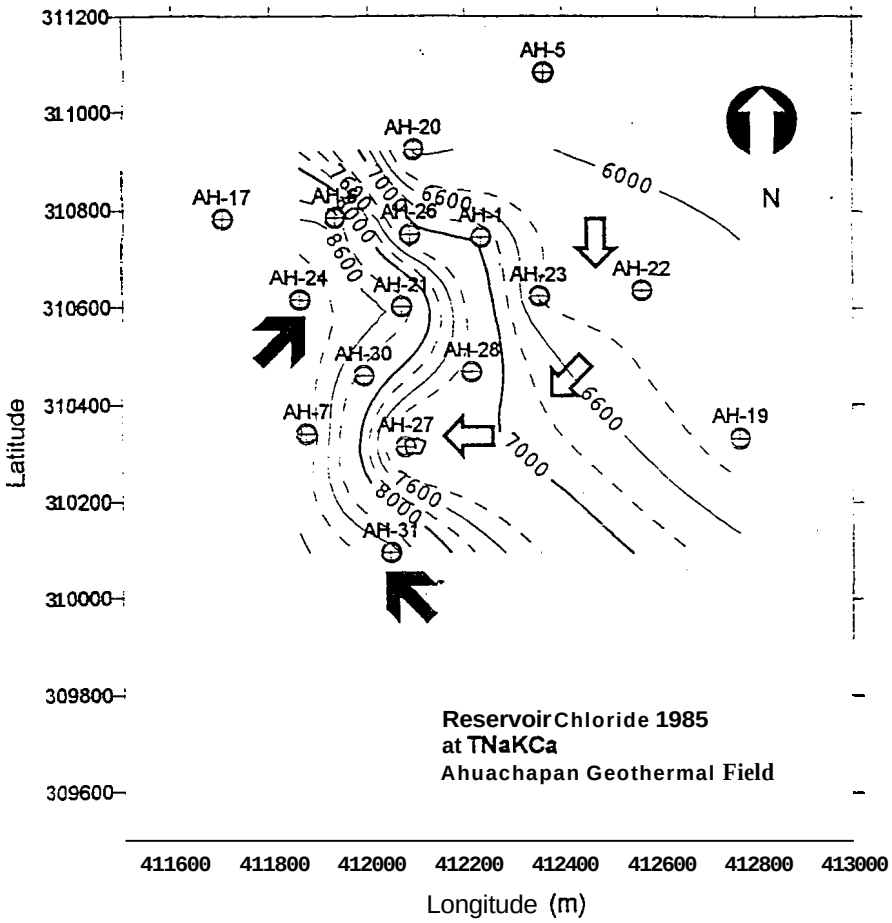

Reservoir chloride distribution in 1985
evaluated from the **NaKCa** geothermometer

Figs. 5 Areal distribution of chloride content in 1985

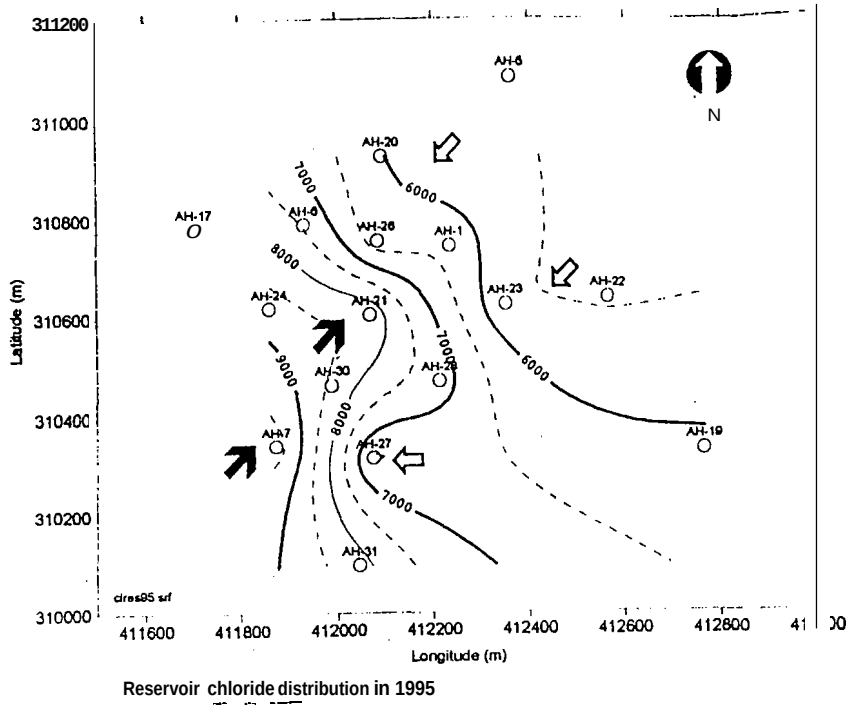

Figs. *6* Areal distribution of chloride content in 1995. It is evident an increasing dilution due to recharge water from E-NE and a resistance to dilution in the W-SW zone, probably close to where the upflow zone is located

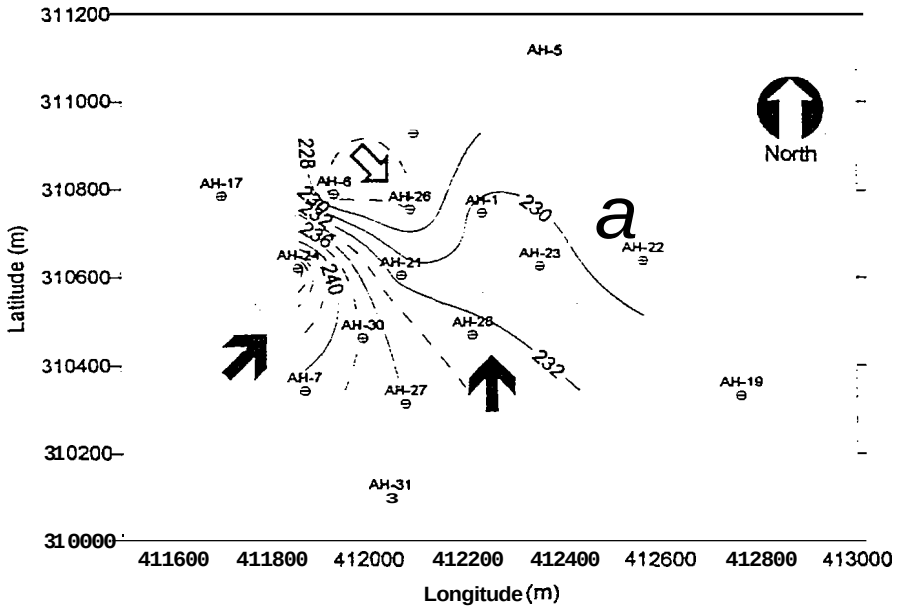

Silica Temperature distribution in 1978
Temperature evaluated from quartz geothermometer (Foumier, 1991)

Figs. 7 Areal distribution of T_{SiO2} at starting conditions.

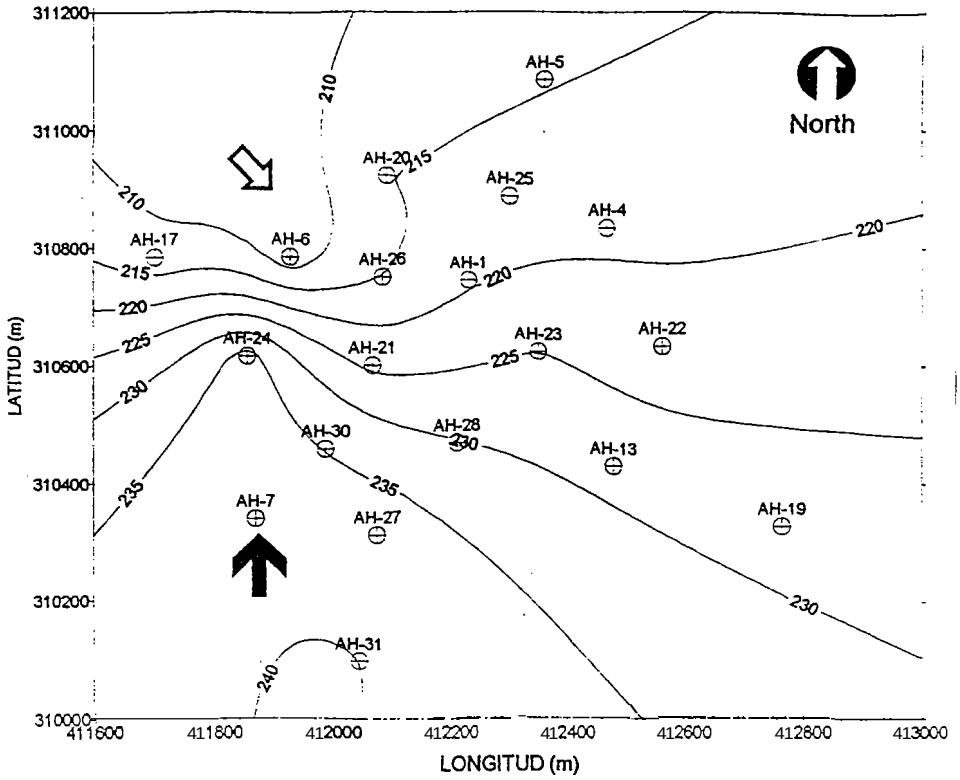

Temperature distribution in 1995.
Temperature evaluated from **quartz** geothennometer (Foumier, 1991).

Figs. 8 Areal distribution of T_{SiO2} in 1995. It.evidences a strong decline in the N-NE zone with the highest computed temperatures in the **S-SW** zone.

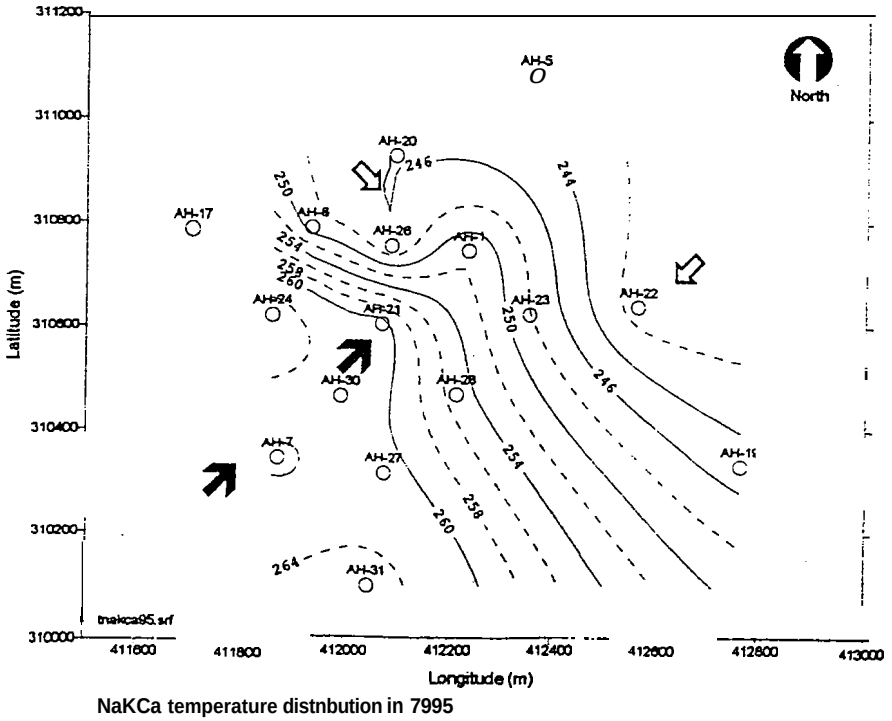

NaKCa temperature distnbution in 7995

Fig. 9 Na-K-Ca temperature dismbution in 1995.

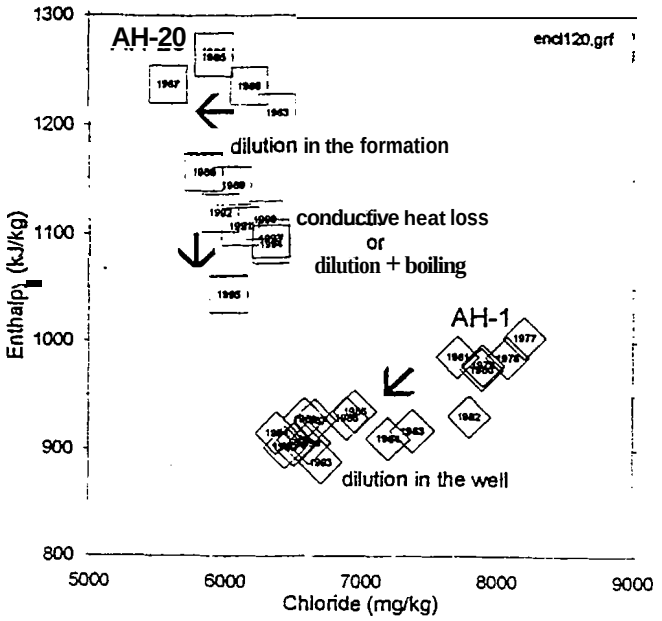

Fig. 10 Enthalpy -chloride diagram for wells *AH-20* and *AH-1*

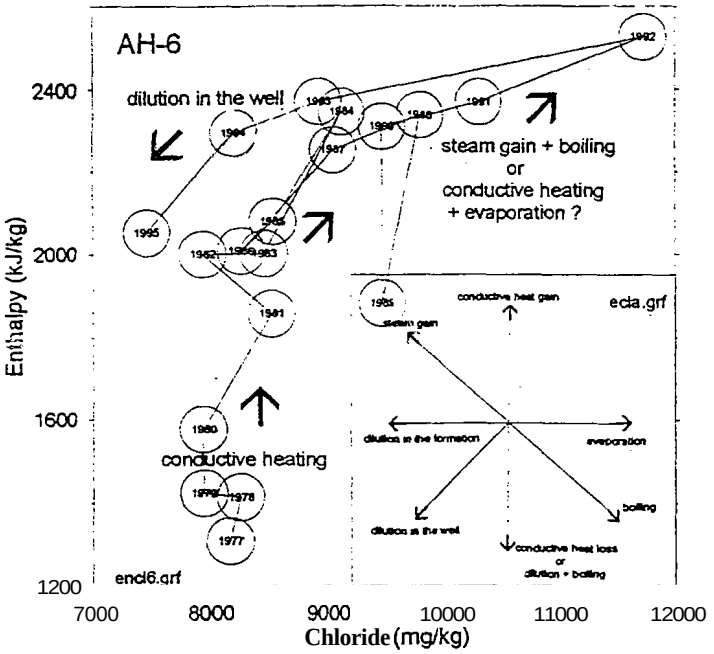

Fig 11 Enthalpy - chloride diagram for well AH-6. Different phenomena can explain the trends with time: conductive heat gain and heat losses (or dilution + boiling) can move the points respectively up or down. Dilution in the formation moves the points on the left at constant enthalpy. Common phenomena at Ahuachapan are steam gain, moving the points up at 45 °, and dilution in the well moving the point down at **45** °. Both phenomena induce dilution represented by a decrease in Cl with respectively an increase and a decrease in enthalpy.

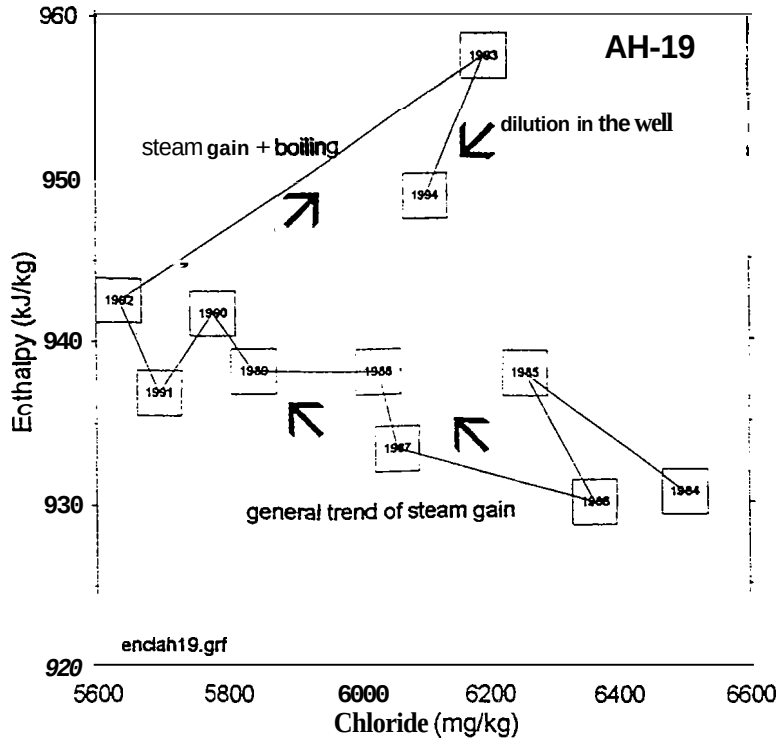

Fig. 12 Enthalpy - chloride diagram for well AH-19.

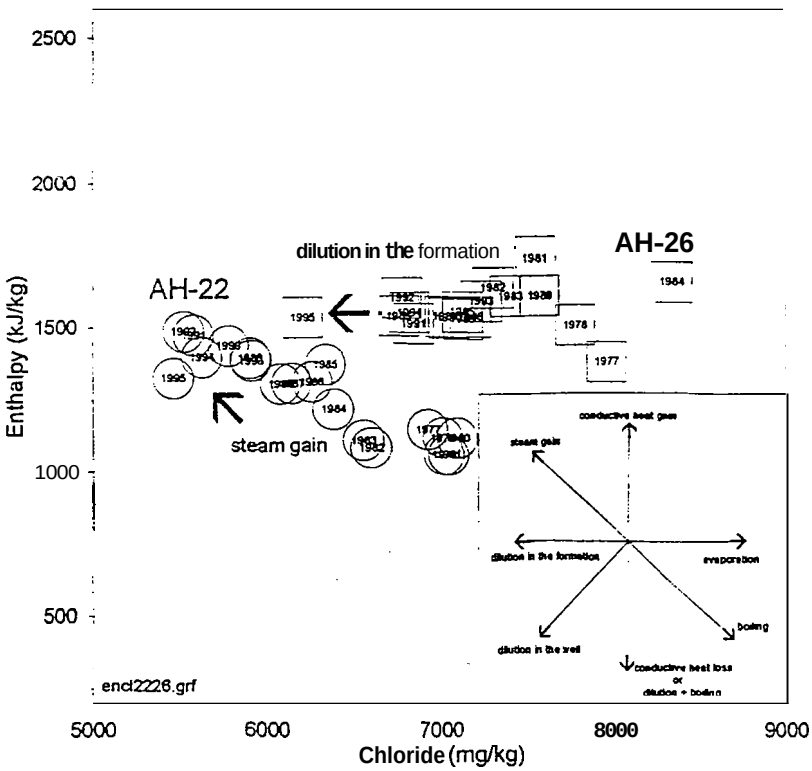

Fig. 13 Enthalpy - chloride diagram for wells AH-22 and AH-26.

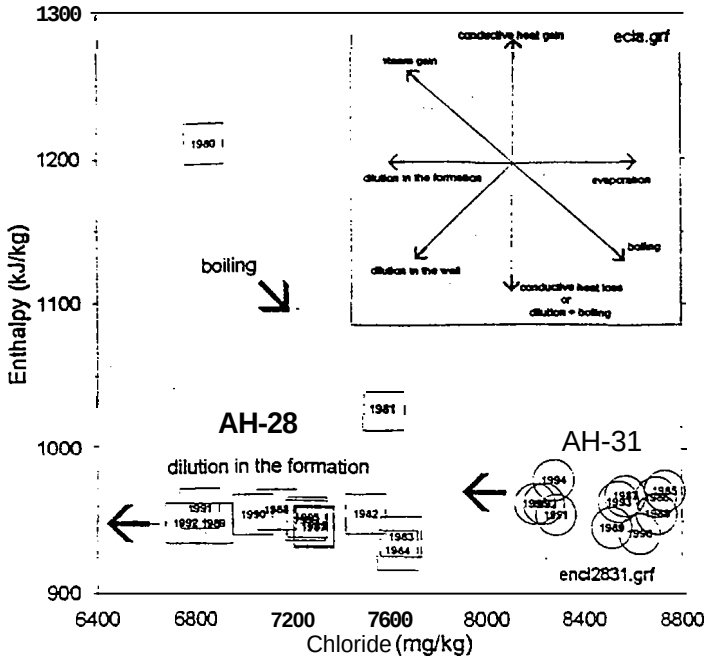

Fig. 14 Enthalpy - chloride diagram for wells AH-31 and AH-2%

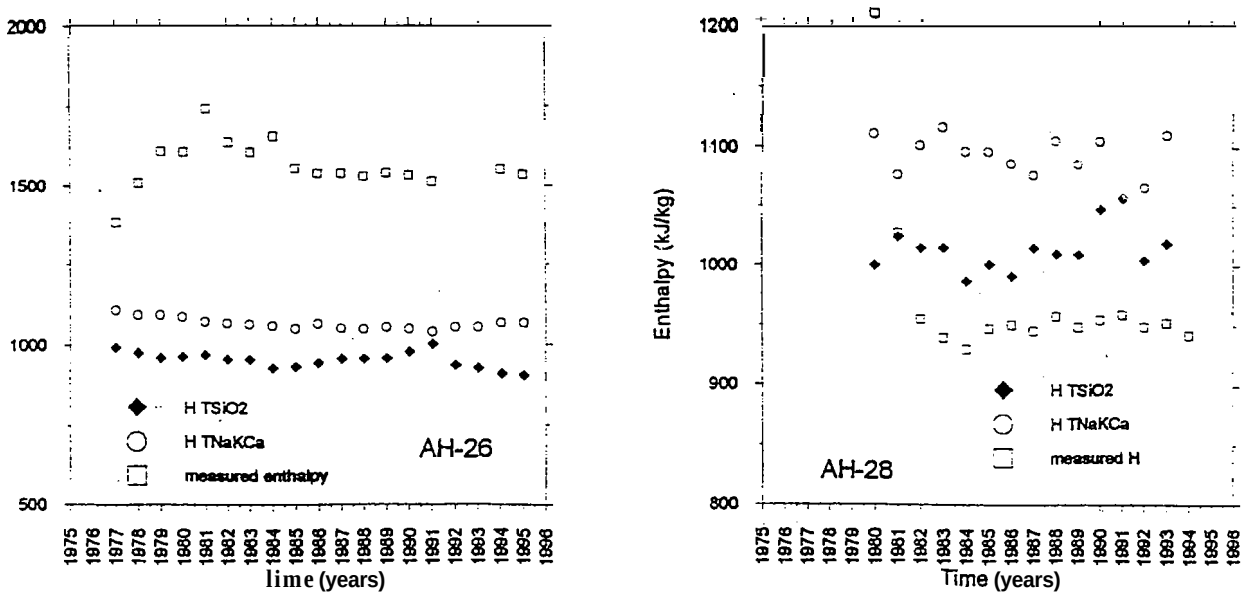

Fig.15 Measured enthalpy and the values of enthalpy for a liquid phase computed from Si02 and Na-K-Ca geothermometers **vs.** time for **wells *AH-26*** and *AH-28.*

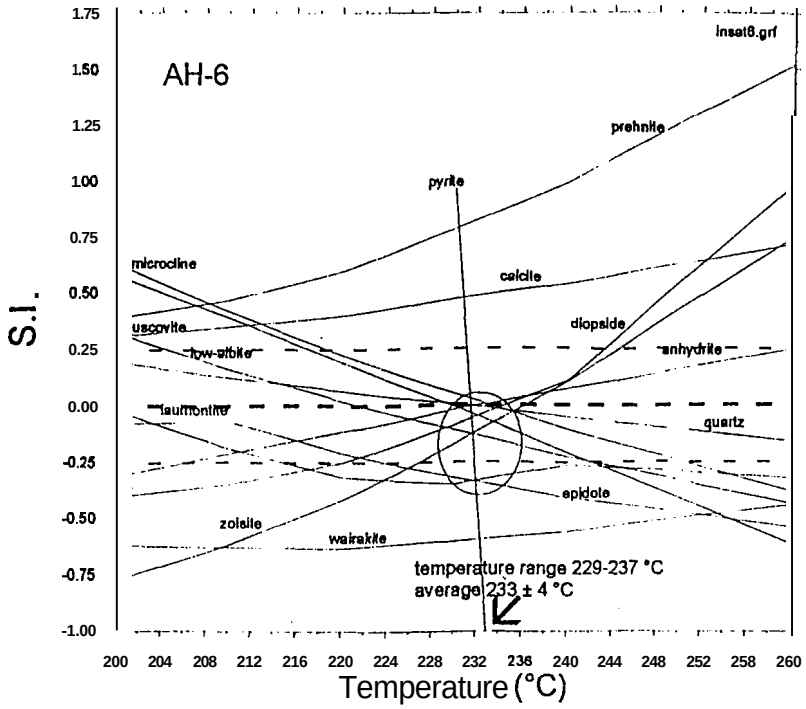

Fig. 16 Values of saturation indexes (SI) **vs** temperature for selected alteration minerals at starting condition for well *AH-6:*

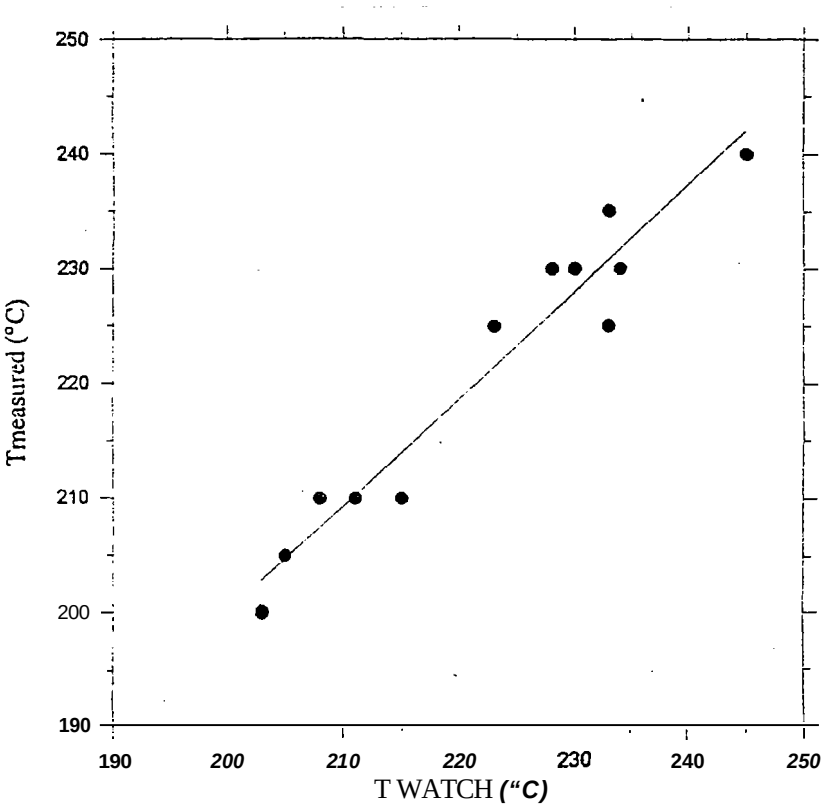

Measured temperature vrs. temperature computed by WATCH code, for six Ahuachapan wells at initial-actual production conditions.

Fig. 17 Correlation between the measured temperatures and the average temperatures computed by the use of saturation indexes.

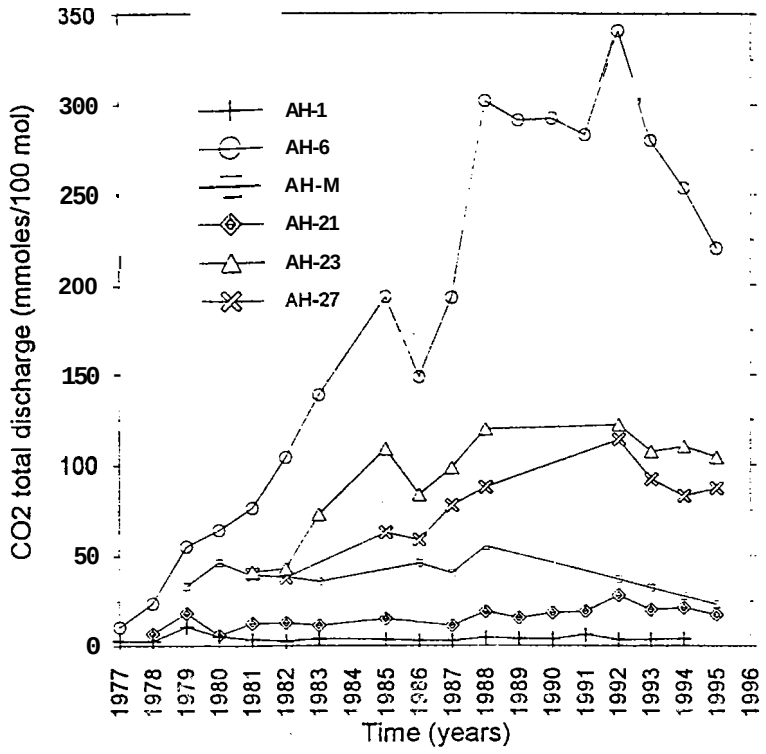

Fig 18 CO_2 in total discharge (mmoles/100 moles) vs time for selected wells.

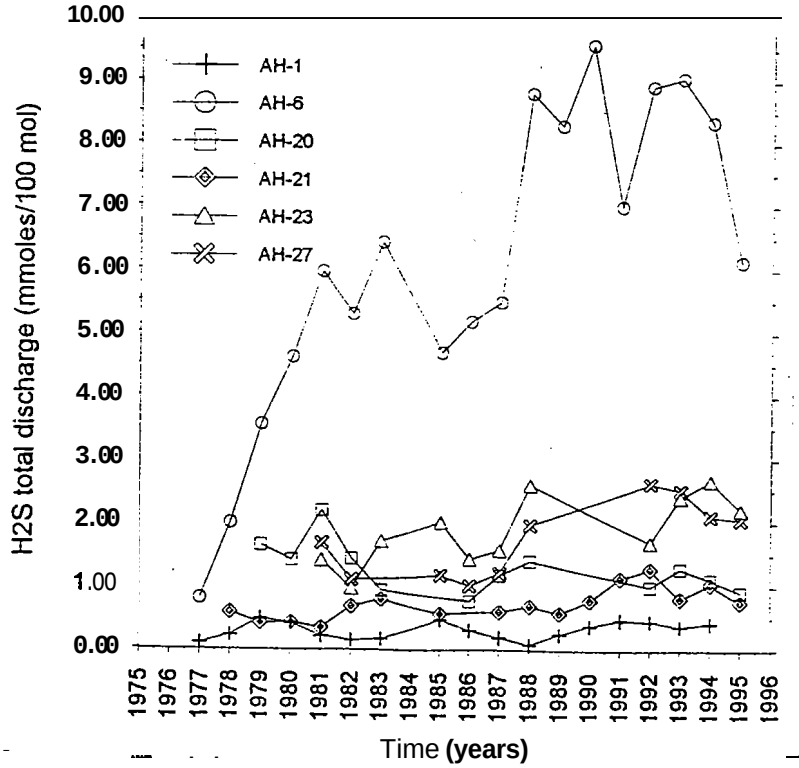

Fig. 19 H_2S in total discharge (mmoles/100 moles) vs time for selected wells.

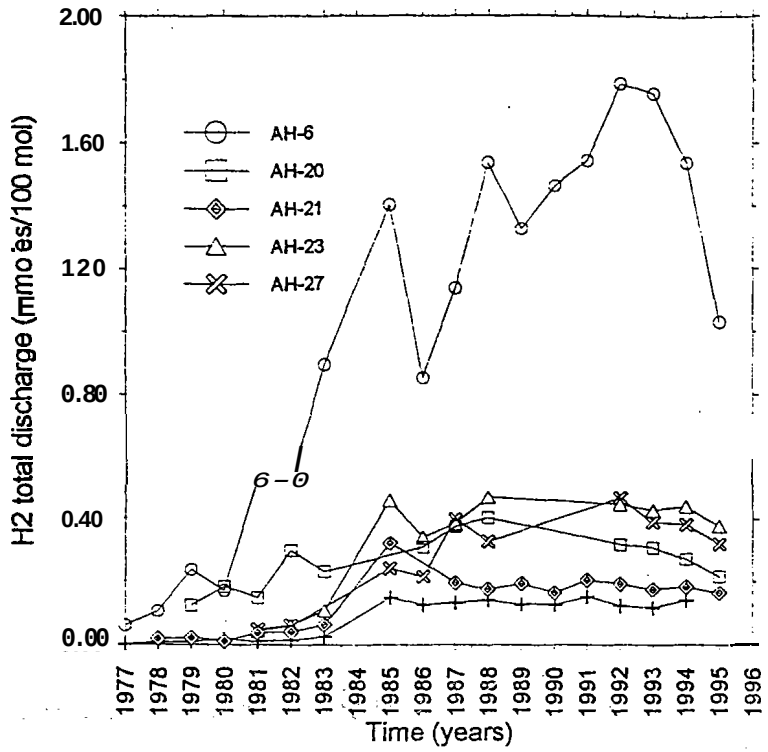

Fig. 20 H_2 in total discharge (mmoles/100 moles) vs time for selected wells.

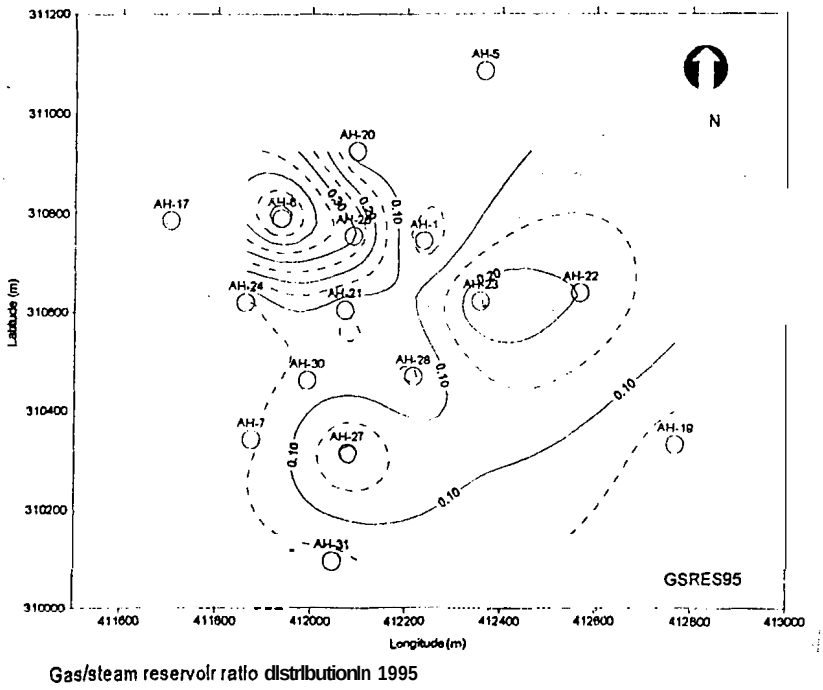

Gas/steam reservoir ratio distribution in 1995

Fig. 21 Gas/H_2O ratio distribution in 1995. Boling points are around wells **AH-6,** AH-23 and **AH-27.**

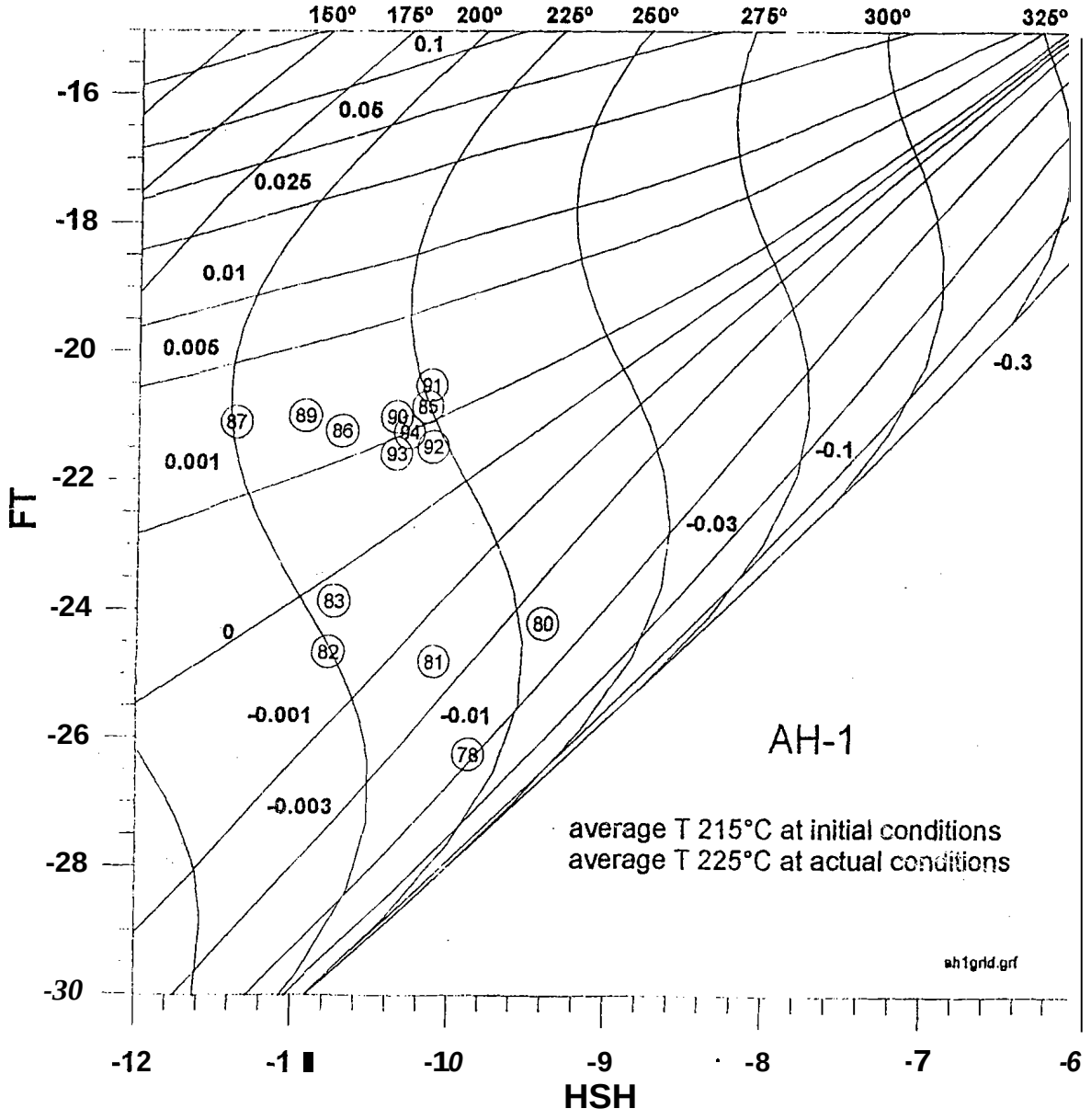

Fig. 22 **Grid** diagrams for gas compositions related to temperature **and** steam fraction *(y)* in the reservoir (D'Amore **and** Truesdell, 1985) for well AH-1.

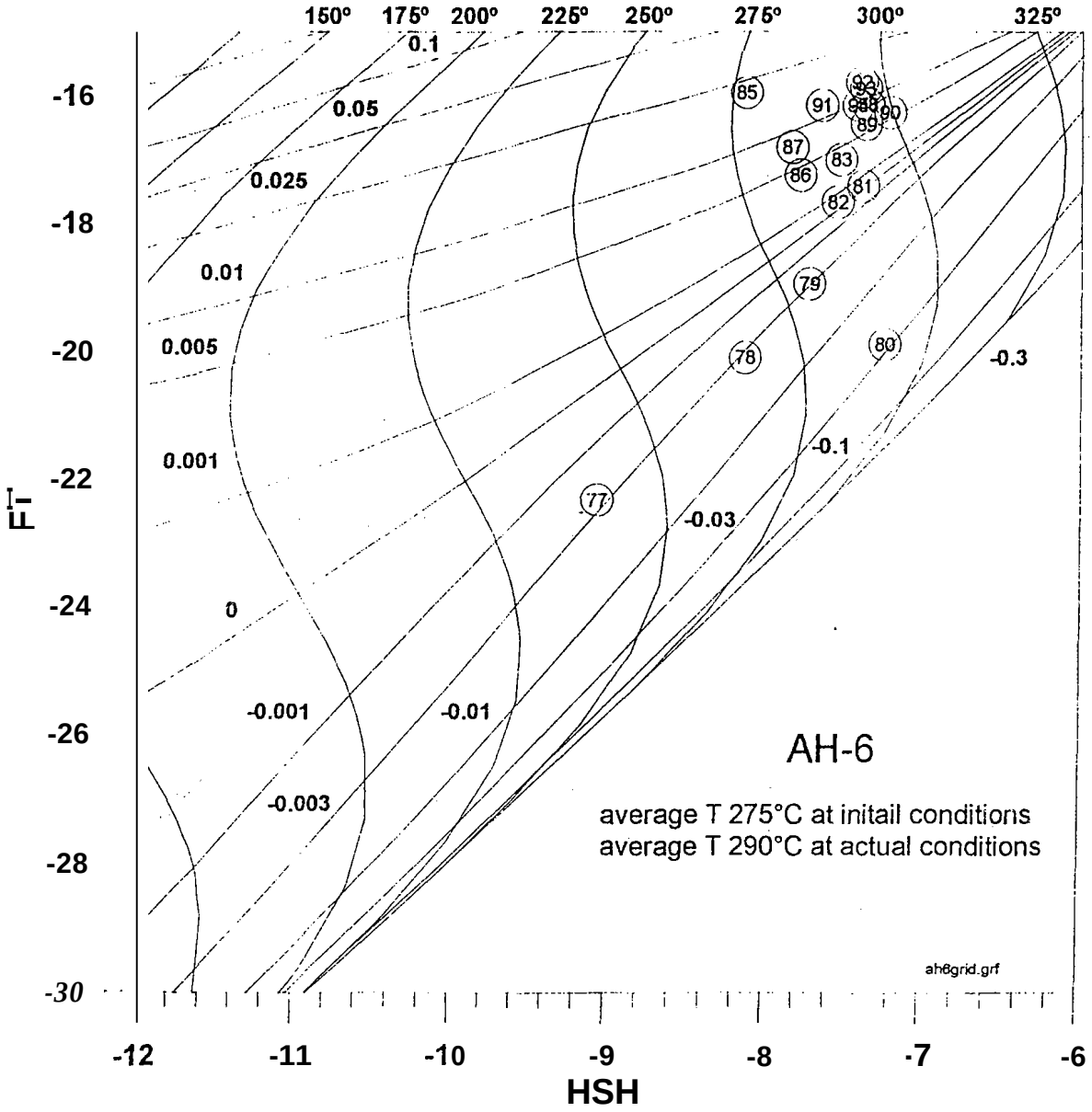

Fig. **23** Grid diagrams for gas compositions related to temperature **and** steam fraction (y) in the reservoir (D'Amore and Truesdell, 1985) for well AH-6.

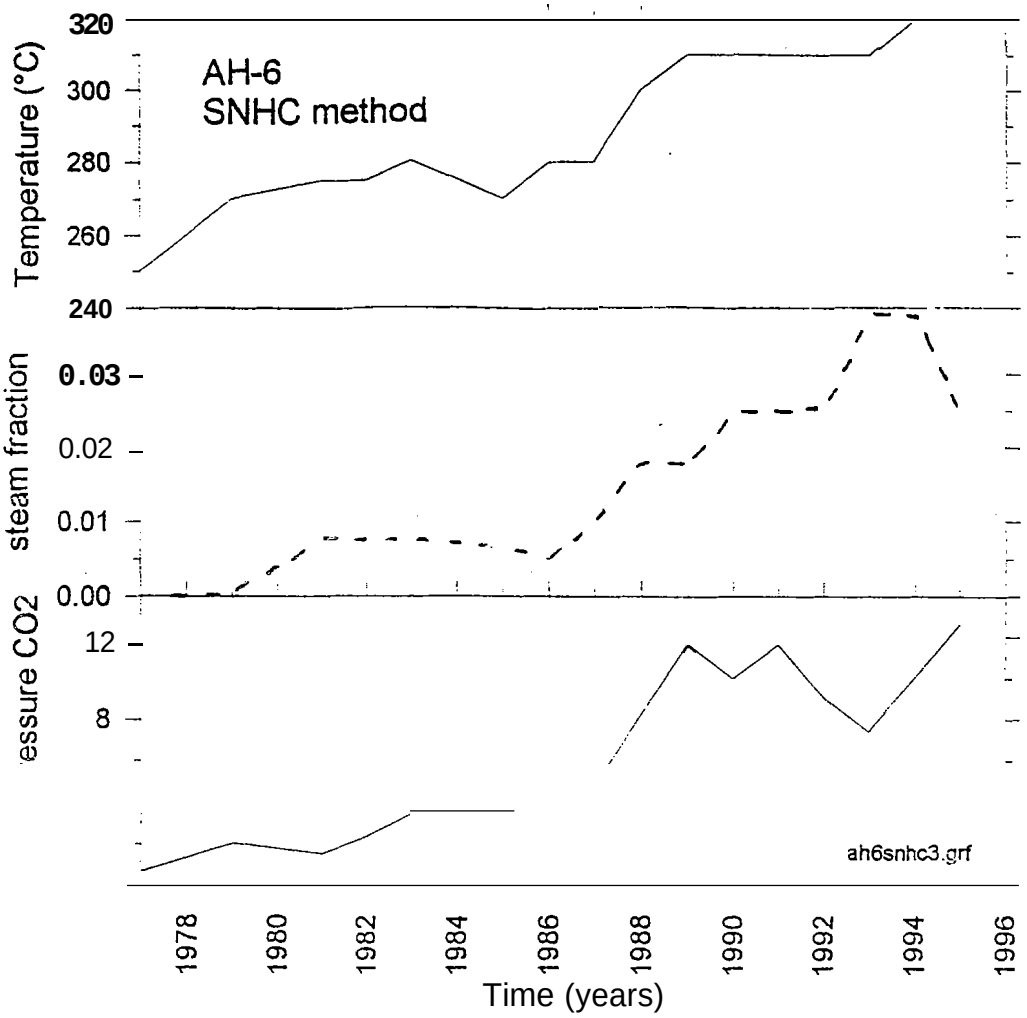

Fig. 24 Values of reservoir euilibration temperature, stem fraction **and** CO_2 partial pressure vs time for well *AH-6* using the method based also on **NH3** and N_2 content (D'Amore **and** Truesdell, 1997, in prep.).

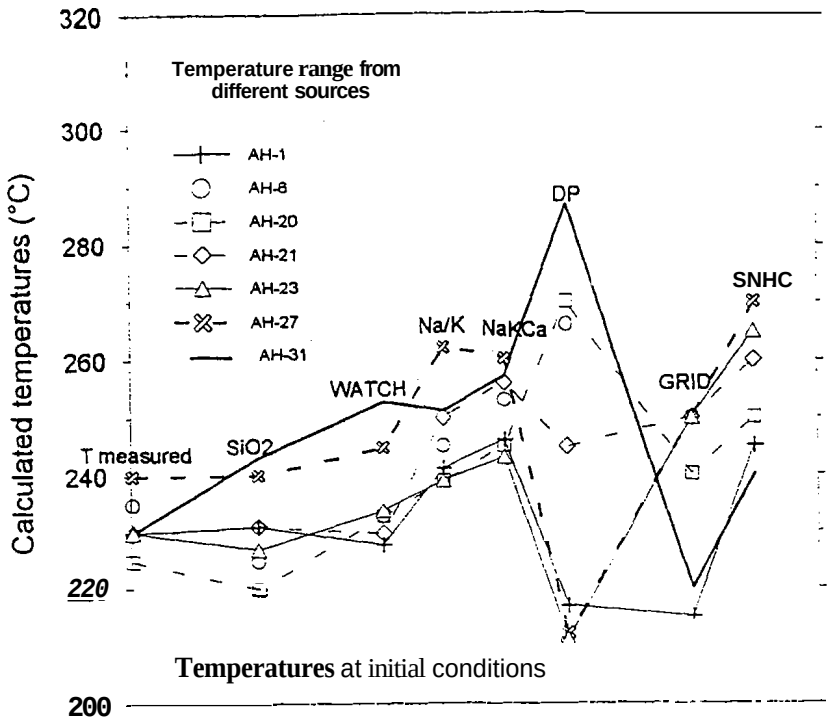

Fig. 25 Temperature range of the values computed from different methods at initial conditions for selected wells.

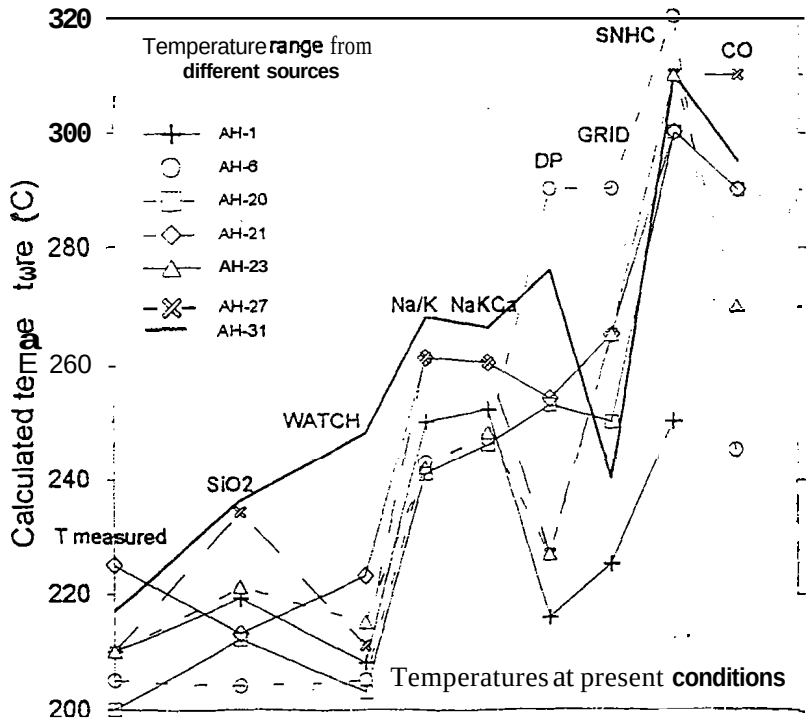

Fig. *26* Temperature range of the values computed from different methods in 1995 for selected wells.

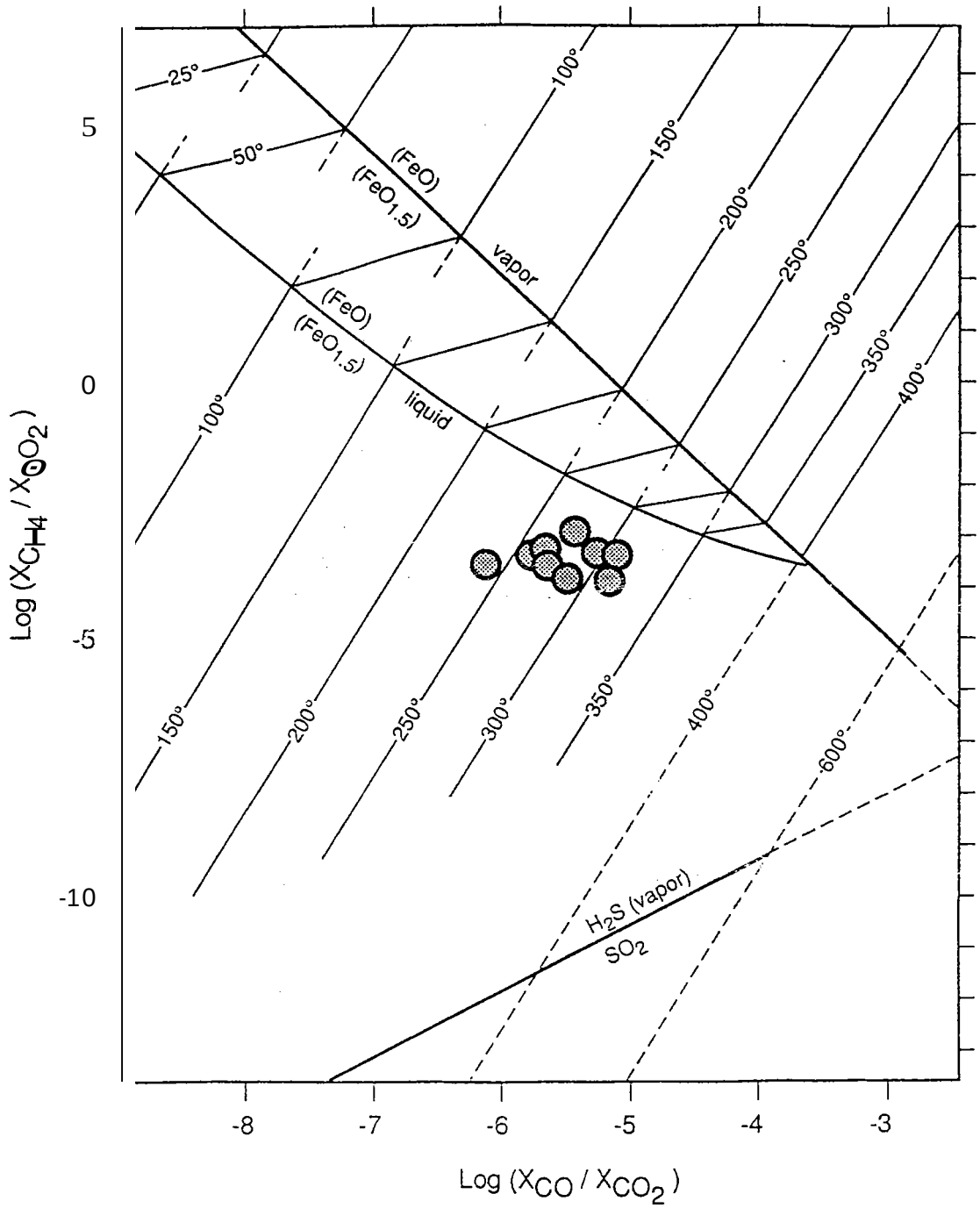

Fig. 27 CO_2-CH_4-CO diagram

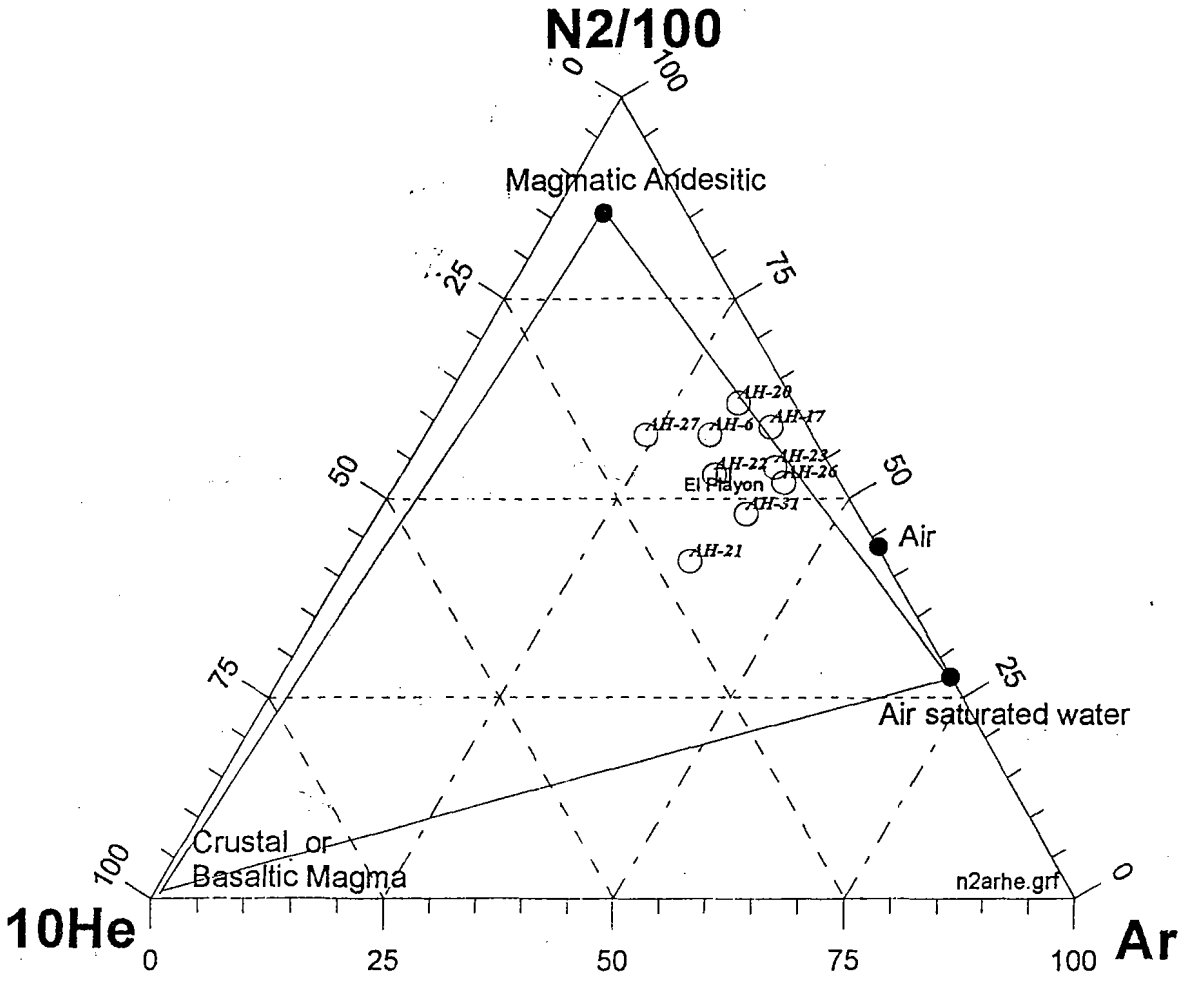

Fig. 28 N_2-Ar-He triangular diagram for the gas of Ahuachapan.

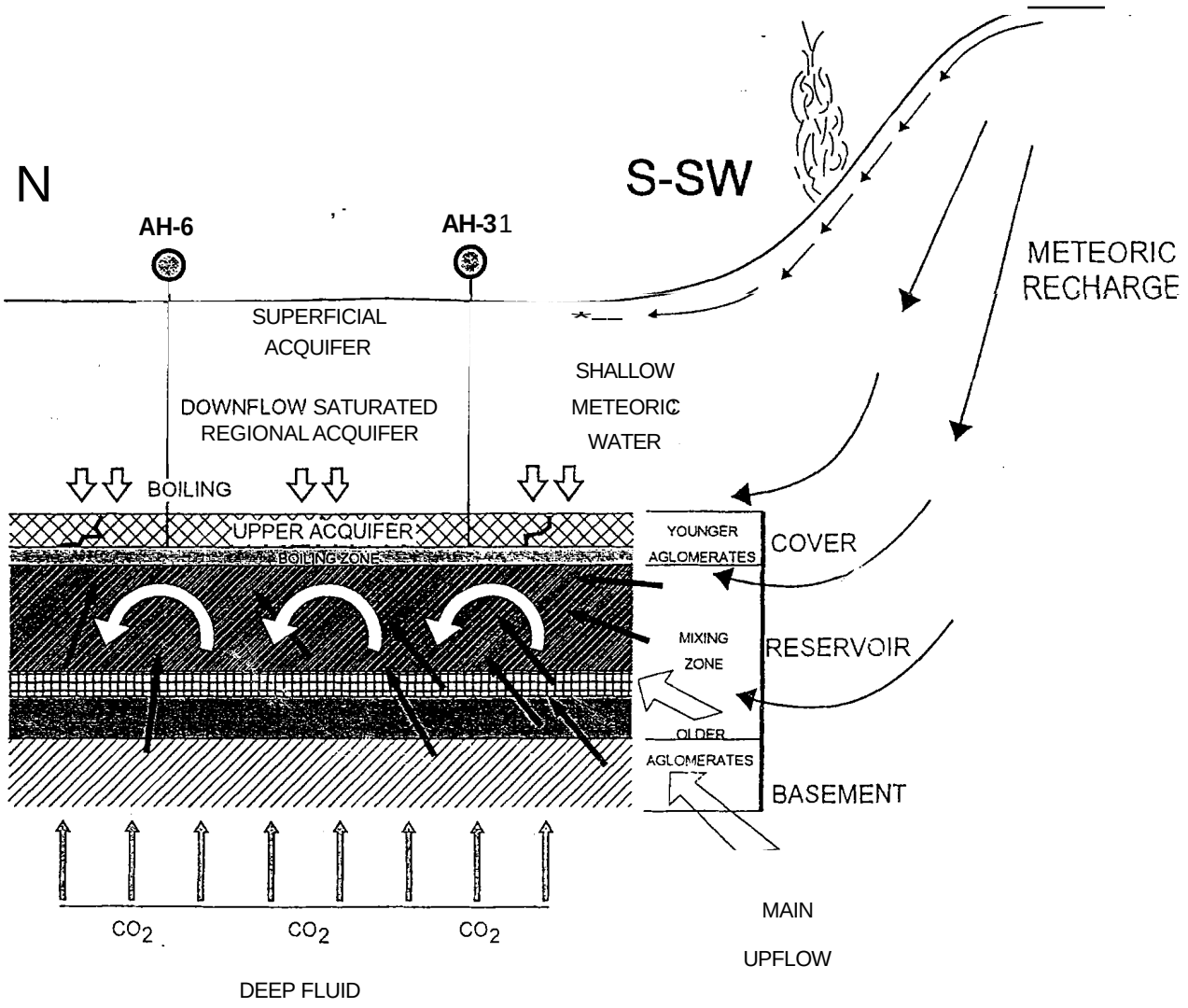

Fig. **29.** Conceptual model of **Ahuachapan** geothermal field.